ACS APPLIED MATERIALS & INTERFACES

Research Article

www.acsami.org

Simultaneously Improving Electrical Conductivity and Thermopower of Polyaniline Composites by Utilizing Carbon Nanotubes as High Mobility Conduits

Hong Wang,[†] Su-in Yi,[†] Xiong Pu,[‡] and Choongho Yu*[,†,‡]

[†]Department of Mechanical Engineering and [‡]Department of Materials Science and Engineering, Texas A&M University, College Station, Texas 77843, United States

ABSTRACT: Electrical conductivity and thermopower of isotropic materials typically have inversely proportional correlation because both are strongly affected in the opposite way by the electronic carrier concentration. This behavior has been one of the major hurdles in developing high-performance thermoelectrics whose figure-of-merit enhances with large thermopower and high electrical conductivity. Here we report a promising method of simultaneously improving both properties with polyaniline (PANI) composites filled by carbon nanotubes (CNTs). With addition of double-wall CNTs (DWCNTs), the electronic mobility of PANI doped with camphorsulfonic acid (PANI-CSA) was raised from ~0.15 to ~7.3 $cm^2/(V\ s)$ (~50 time improvement) while the carrier concentration was decreased from ~2.1×10^{21} to ~5.6×10^{20} cm^{-3} (~4 time reduction). The larger increase of mobility increased electrical conductivity despite the carrier concentration reduction that enlarges thermopower. The improvement in the carrier mobility could be attributed to the band alignment that attracts hole carriers to CNTs whose mobility is much higher than that of PANI-CSA. The electrical conductivity of the PANI-CSA composites with 30-wt % DWCNTs was measured to be ~610 S/cm with a thermopower value of ~61 μV/K at room temperature, resulting in a power factor value of ~220 $\mu W/(m\ K^2)$, which is more than two orders higher than that of PANI-CSA as well as the highest among those of the previously reported PANI composites. Further study may result in high performance thermoelectric organic composites uniquely offering mechanical flexibility, light weight, low toxicity, and easy manufacturing. unlike conventional inorganic semiconductors.

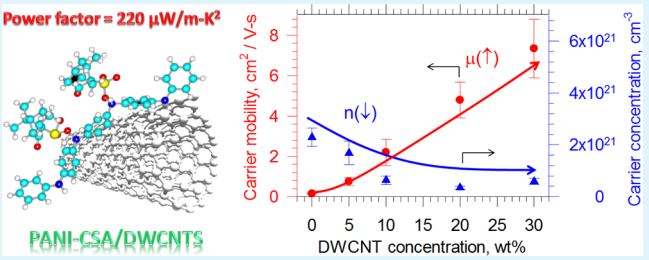

KEYWORDS: *thermoelectric, polyaniline, simultaneous improvement, carbon nanotube composites, mobility, carrier concentration*

1. INTRODUCTION

Thermoelectric cooling and energy harvesting are suited to the applications that require small dimensions and silence without moving parts and working fluids,[1] which often make thermoelectric devices unique solutions (e.g., optoelectronics cooling and mobile systems). While conventional thermoelectric materials such as tellurium, lead, and bismuth are heavy, brittle, toxic, and expensive, diminishing the benefit of thermoelectric devices, organic thermoelectric materials could be flexible, nontoxic, and inexpensive options for operations near room temperature. However, organic materials typically have relatively poor electrical conductivity (σ) and thermopower (or the Seebeck coefficient) (S), which make up the thermoelectric power factor ($S^2\sigma$) that indicates the capability of power generation and cooling. For example, polyaniline (PANI) has recently been studied for thermoelectric applications but thermoelectric power factors of PANI only films are very small, which are typically in the range of 0.001−1 $\mu W/(m\ K)^2$.[2,5−7]

To overcome the drawbacks, there have been efforts to make composites with conducting fillers in host polymer matrices. For example, electrically conducting inorganic materials or conventional thermoelectric materials such as Bi_2Te_3, PbTe, and Au nanoparticles were embedded in polymers.[8−14] Although there has been progress, the power factor is still small, 0.01−50 $\mu W/(m\ K^2)$. Moreover, the inorganic fillers are likely to negate the major benefit of organic materials such as mechanical flexibility, lightweight, and nontoxicity.

On the other hand, carbon-based materials such as CNTs, graphene, and graphite were also studied as fillers owing to their high electrical conductivity and flexibility.[15−18] In particular, one-dimensional CNTs are excellent candidates because it is possible to improve the electrical conductivity of composites with a small concentration of CNTs due to a low critical volume fraction at percolation.[19,20] It was demonstrated that the thermoelectric properties of CNTs can be controlled to have higher power factor[21−24] or/and both n-type and p-type behaviors.[25−27] Recent papers have also shown that addition of conductive fillers to polymers can improve the power factor by increasing electrical conductivity with relatively constant thermopower.[20,28−31] While composites made of poly(3,4-ethylenedioxythiophene) (PEDOT) and CNTs show relatively

Received: February 5, 2015
Accepted: April 20, 2015
Published: April 20, 2015

DOI: 10.1021/acsami.5b01149
ACS Appl. Mater. Interfaces 2015, 7, 9589−9597

high power factors,[28−31] most of PANI/CNT composites have orders of lower power factors (<50 μW/(m K^2)).[15,32,33] A large improvement for PANI/CNT composites was reported in a very recent paper (176 μW/(m K^2)),[34] but this is still inferior to those of PEDOT/CNT composites.

In this paper, we report simultaneous improvement of both electrical conductivity and thermopower, which resulted in a large enhancement in the power factor. The highest power factor was measured to be ∼220 μW/(m K^2), which is the highest among those of the previously reported PANI composites.[2,4,9,15−18,32−43] This large improvement could be attributed to the increase of electronic carrier mobility for higher electrical conductivity and the reduction of the electronic carrier concentration for larger thermopower. The following describe synthesis and characterization of the composites and their electronic properties.

2. MATERIALS AND METHODS

2.1. Materials. We used PANI emeraldine base (PANIeb) or PANI doped with camphorsulfonic acid (PANI-CSA) (99%, Alfa Aesar) together with single/double-wall CNTs (S/DWCNTs) (99 wt %, Cheaptubes) or DWCNTs (99.9 wt %, Continental Carbon Nanotechnology). PANIeb ($[(C_6H_4NH)_2(C_6H_4N)_2]_n$) with 99.9% purity and a molecular weight of ∼50 000 (Sigma-Aldrich), and CSA (99%, Alfa Aesar) and *m*-cresol (99%, Alfa Aesar) were used for synthesizing PANIeb and CSA-doped PANI composites.

2.2. Sample Preparation. An *m*-cresol solution containing 1 wt % PANIeb was prepared with 0.5 g of PANIeb and 34 mL of *m*-cresol by using a pen-type sonicator (Misonix Microson XL2000, 10 W for 30 min). Another 1.4-wt % PANI-CSA solution was prepared by mixing 0.5 g of PANIeb and 0.64 g of CSA in 35 mL of *m*-cresol with the pen-type sonicator (20 W) for 30 min. Undissolved particles (less than ∼1 wt % of PANIeb powders) in the PANIeb and PANI-CSA solutions were removed by using polytetrafluoroethylene filters (pore size is 0.45 μm). CNT solutions were prepared by sonicating 20-mg S/DWCNTs or DWCNTs in 34 mL of *m*-cresol with the pen-type sonicator (10 W) for 30 min. Subsequently, these solutions were homogenized by an additional 20 h sonication in a bath-type sonicator (Branson 1510).

The CNT solutions were mixed with the PANIeb or PANI-CSA solution with different ratios to have 18 different variations of the solid contents in the composites for this study (Table 1 and Figure 1a, b). The mixture was homogenized in the ultrasonic bath for additional 20 h. The solution was dropped on glass substrates and dried at 40 °C on a hot plate until the solution was fully dried (typically ∼20 h) in an ambient condition. The film thickness was measured to be 3.5−19 μm with 1 mL of the solution on 2 × 2 cm^2 glass substrates, depending on the solid contents in the solution. The dried films were then annealed at 100 °C for 2 h in a vacuum (∼0.1 Torr) for densification. PANI composite films are black and flexible like Figure 1c.

Table 1. List of Samples Containing Different Types of PANI and CNT with Various CNT Concentrations

sample no.	PANI type	CNT type	CNT concentration (wt %)
1	PANIeb	S/DWCNT	50
2	PANIeb	S/DWCNT	75
3	PANIeb	S/DWCNT	83.3
4	PANI-CSA	S/DWCNT	9.1
5	PANI-CSA	S/DWCNT	16.7
6	PANI-CSA	S/DWCNT	28.6
7	PANI-CSA	S/DWCNT	50
8	PANI-CSA	S/DWCNT	66.7
9	PANIeb	DWCNT	5
10	PANIeb	DWCNT	10
11	PANIeb	DWCNT	20
12	PANIeb	DWCNT	30
13	PANI-CSA	DWCNT	0.1
14	PANI-CSA	DWCNT	1
15	PANI-CSA	DWCNT	5
16	PANI-CSA	DWCNT	10
17	PANI-CSA	DWCNT	20
18	PANI-CSA	DWCNT	30

S/DWCNT-only and DWCNT-only samples were also prepared by drop-casting solutions containing S/DWCNT (0.1 wt %) and sodium dodecylbenzenesulfonate (SDBS) (0.5 wt %) in 1−1.5 mL of *m*-cresol. Prior to the drop casting process, the solution was homogenized by using the bath-type sonicator for 24 h. The obtained film was dried at 40−50 °C on a hot plate in an ambient condition until the solution was fully dried (typically for ∼20 h). The dried films were then annealed at 100 °C for 2 h in vacuum (∼0.1 Torr) to improve electrical conductivity. The film thickness was measured to be ∼1 μm with 1 mL of the solution on 2 × 2 cm^2 glass substrates.

2.3. Characterization. Scanning electron micrographs (SEMs) of composite were taken with an FEI Quanta 600 FE-SEM. To obtain the highest occupied molecular orbital (HOMO) and the lowest unoccupied molecular orbital (LUMO), we carried out cyclic voltammetry (CV) experiments (CHI 600 workstation) with a Pt wire as a counter electrode and a silver wire as a pseudoreference electrode in a standard one-compartment and three-electrode cell. Spin-coated samples on a glassy carbon electrode were used as a working electrode. An anhydrous acetonitrile solution (99.8%, Sigma-Aldrich) containing 0.1-M Bu_4NPF_6 (98%, Sigma-Aldrich) and 0.01-M $AgNO_3$ (99.9%, Alfa Aesar) was used as an electrolyte. Before testing, the solution was bubbled with Ar for 20 min to remove oxygen. HOMO and LUMO were determined from the onset potentials of oxidation and reduction by assuming the energy level of ferrocene/ferrocenium (Fc/Fc^+) is −4.8 eV.[27] The half wave potential of Fc/Fc^+ was measure to be 0.0 V against Ag/Ag^+ in the electrolyte used for all experiments. The Fermi level or work function (WF) of the samples was determined by the Kelvin probe method with an atomic force microscope (AFM) (Dimension Icon, Bruker) and a Pt-coated tip (OSCM-PT model, Bruker). After the contact potential difference (CPD) between the AFM tip and the samples was measured, WF was calculated with following equation:[27] $WF_{sample} = WF_{tip} - CPD$. Before measurement, the WF of the tip was calibrated with a pure gold foil (99.95%, 0.05 mm in thickness, Alfar Aesar), whose work function was assumed to be 5.1 eV.

Electrical conductivity and thermopower of the composites were measured at room temperature along the in-plane direction of the films with a multimeter (Keithley 2000) and a data acquisition system programmed by Labview (National Instruments). A four-probe current−voltage measurement method was employed to accurately determine the electrical conductivity. Current from 0 to ±1 mA was passed to the sample to acquire a slope from a linear current−voltage curve. For thermopower measurements, voltage values across a sample were measured at 6 different temperature gradients between −3 and +3 K. Thermopower was obtained from the slope of a linear temperature−voltage curve. The coefficient of determination for finding the slope in the measurement was greater than 0.99. For each data point, four or more samples were tested to obtain the standard deviation (std), which was calculated by using the following relations.

$$\text{std} = [\sum_{i=1}^{n} (X_i - X_m)^2/n]^{0.5} \text{ and } X_m = \sum_{i=1}^{n} X_i/n$$

where X_i and n are experimental data and the number of samples, respectively. Hall measurements were performed according to ASTM F76−08 to obtain the electronic carrier mobility and concentration. With the van der Pauw geometry with 1 cm × 1 cm square samples, sheet resistances and Hall voltages were measured under 1 T.

3. RESULTS AND DISCUSSION

SEMs in Figure 2 show Sample 1 containing PANIeb with 50-wt % S/DWCNTs has rough surfaces with nanoscale pinholes

DOI: 10.1021/acsami.5b01149
ACS Appl. Mater. Interfaces 2015, 7, 9589−9597

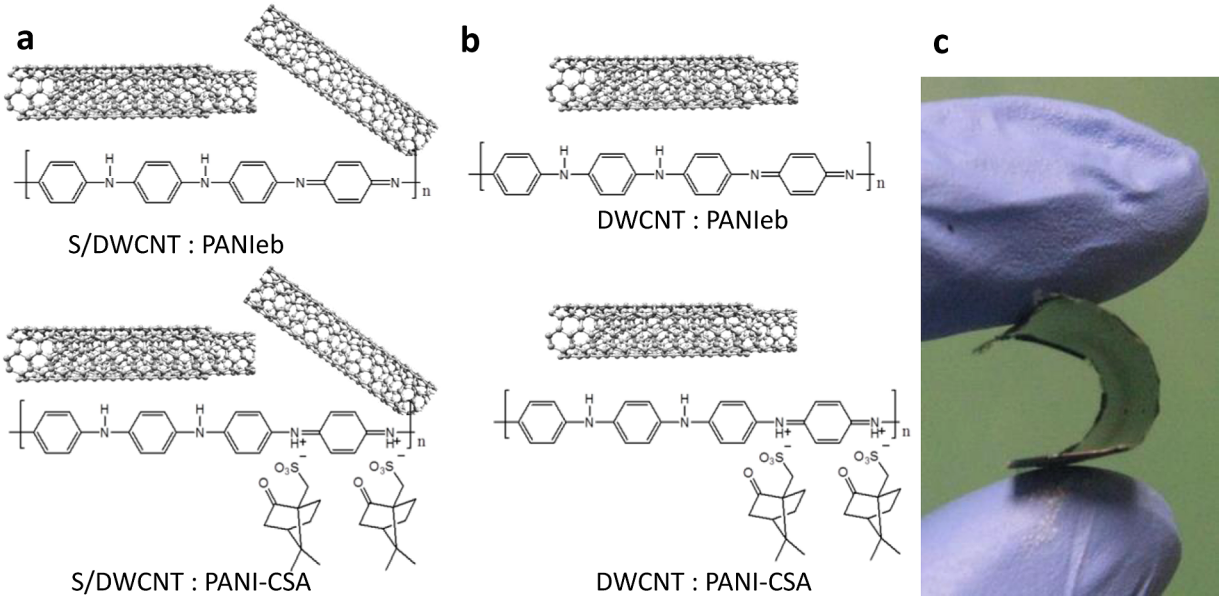

Figure 1. Four different sets of composites were synthesized by drop-casting mixture solutions of CNT and PANI. (a) S/DWCNT composites with PANIeb or PANI-CSA. (b) DWCNT composites with PANIeb or PANI-CSA. (c) Composite containing 30 wt % DWCNTs with PANI-CSA (deposited on a plastic film), demonstrating its flexibility.

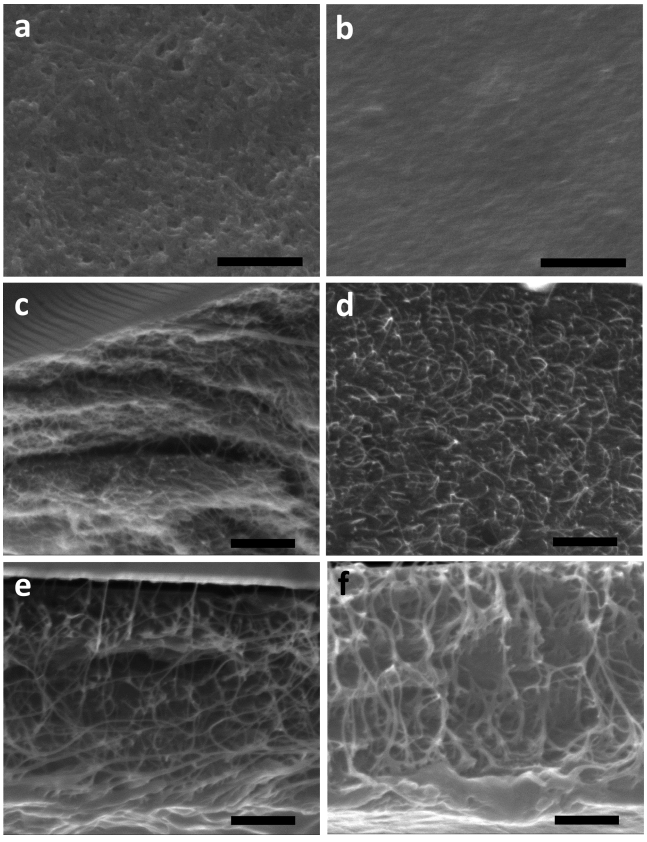

Figure 2. Top surface of (a) a PANIeb film (Sample 1) and (b) a PANI-CSA film (Sample 7) containing 50-wt % S/DWCNTs. The fractured cross-sections along the out-of-plane direction of (c) Sample 1 and (d) Sample 7, and those of (e) a PANIeb film (Sample 11) and (f) a PANI-CSA film (Sample 17) containing 30-wt % DWCNTs. All scale bars indicate 1 μm.

(Figure 2a), compared to Sample 7 (PANI-CSA with 50-wt % S/DWCNTs) whose surface is smooth (Figure 2b). Their cold-fractured cross sections (Figure 2c,d) indicate that more and longer CNTs were pulled out from the surface of the PANIeb composite compared to PANI-CSA. This implies that adhesion between the CNTs and PANIeb is inferior to that of the PANI-CSA composites presumably because of the rigid structure of PANIeb compared to PANI-CSA. In fact, when PANIeb composites were synthesized with a lower concentration of S/DWCNTs, the composites easily cracked despite the enhanced mechanical property by CNTs. This is why the CNT concentrations in PANIeb composites are high compared to PANI-CSA composites (see Table 1). We believe the rigid structure made the composites brittle, and cracks were caused by shrinkage during the drying process.

The irregularly fractured surface from the PANIeb composite is also another indication of poor and nonuniform adhesion between the CNTs and PANIeb. It appears that the CSA doping has a plasticizing effect, which might be due to a lower crystallinity caused by the CSA molecules attached to the backbone. Similar differences were observed from Sample 12 (Figure 2e) and Sample 18 (Figure 2f) containing 30 wt % DWCNTs. DWCNTs contain less impurity particles compared to S/DWCNTs,[22] which may result in a higher packing density as well as better adhesion between DWCNTs and PANI. We believe this allowed us to synthesize composites with much lower DWCNT concentrations.

The electrical conductivity, thermopower, and power factor of Sample 1−3 (PANIeb with S/DWCNT) and Sample 4−8 (PANI-CSA with S/DWCNT) are depicted in Figure 3a and 3b, respectively. The electrical conductivity of the PANIeb composite with 50-wt % S/DWCNTs was measured to be only 4.7 S/cm, which is much lower than that of PANI-CSA composites with 50-wt % S/DWCNTs. We believe this is because electronic transport across the junctions between CNTs is deterred by the electrically resistive PANIeb, as conceptually illustrated in the inset of Figure 3b. The electrical conductivity of the PANIeb composite was improved by raising the S/DWCNT concentration while thermopower was suppressed. This opposite behavior is typical in bulk semi-

DOI: 10.1021/acsami.5b01149
ACS Appl. Mater. Interfaces 2015, 7, 9589−9597

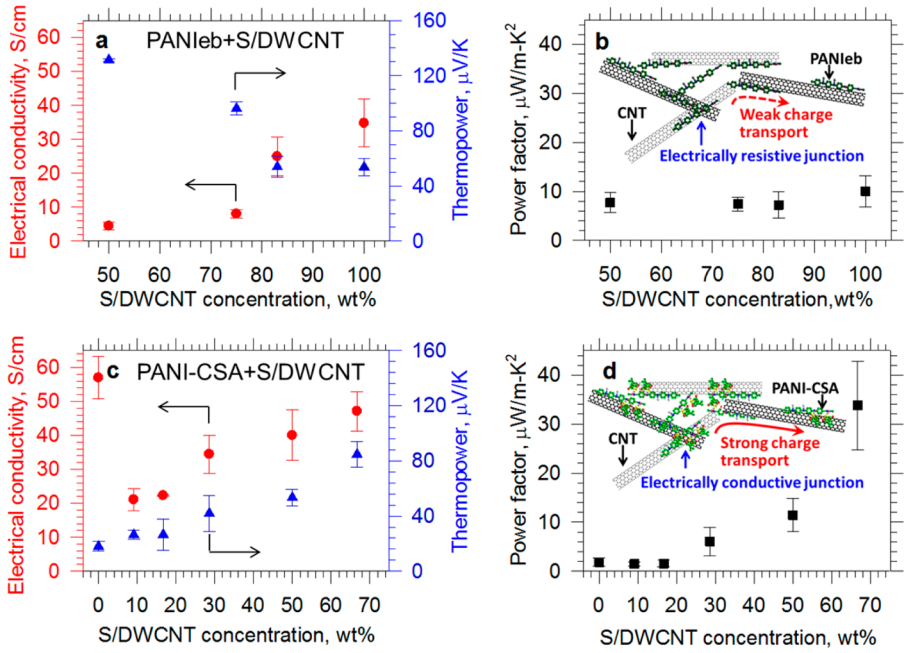

Figure 3. Electrical conductivity and thermopower of (a) PANIeb composites (Sample 1−3) and (c) PANI-CSA composites (Sample 4−8) containing various amounts of S/DWCNTs. An S/DWCNT-only sample was also displayed for comparison. The corresponding power factors for (b) PANIeb composites and (d) PANI-CSA composites. The insets illustrate that CNTs are connected by electrically resistive (b) PANIeb deterring charge transport and (d) PANI-CSA serving as electrically conducting glue to facilitate charge transport at the junctions between CNTs.

conductors when the electronic carrier concentration is increased, but here we increased the CNT concentration. The electrical conductivity of the S/DWCNT only films (0 wt % PANI) was measured to be ~35 S/cm, which is much lower than the values of previously reported CNT only films. For example, when CNT films were prepared with different dispersants (*N*-methyl-2-pyrrolidone or SDBS with water), the electrical conductivity of the films with similar CNTs (synthesized by a chemical vapor deposition method) was measured to be ~200 S/cm.[22]

The relatively low electrical conductivity of the S/DWCNT only films may come from inferior CNT dispersions in *m*-cresol as well as electrically insulating *m*-cresol leftovers and/or SDBS in the sample. It should be noted that the nanotube dispersion can dramatically alter electrical conductivity[22] because it affects the energy barrier and the number of tube−tube junctions for charge transport. Another reason for the lower electrical conductivity of the S/DWCNT only film might be the low density of nanotube networks because it was prepared by using a drop-casting method compared to a vacuum filtering method[22,26,27] used for the sample with the higher conductivity.

With 50 wt % S/DWCNTs, the composite had a relatively high thermopower value of ~131 μV/K. When the concentration of S/DWCNTs was increased to 83.3 wt %, the thermopower dropped to ~54 μV/K, which is similar to that of the S/DWCNT only sample. This decreasing thermopower values for Sample 1−3 (Figure 3a) as a function of CNT concentration could be qualitatively understood as follows. Assuming that the composite is made of two parallel PANIeb and S/DWCNT resistors, the thermopower of the composite can be described as

$$S_{composite} = \frac{S_{PANIeb}/R_{PANIeb} + S_{CNT}/R_{CNT}}{1/R_{PANIeb} + 1/R_{CNT}} = \frac{S_{PANIeb}}{1 + R_{PANIeb}/R_{CNT}} + \frac{S_{CNT}}{R_{CNT}/R_{PANIeb} + 1} \quad (1)$$

where R_{PANIeb}, R_{CNT}, S_{PANIeb}, and S_{CNT} are the electrical resistances and thermopowers of PANIeb and S/DWCNTs, respectively. When the concentration of S/DWCNTs is raised, R_{CNT} decreases and R_{PANIeb} increases (i.e., $1 + R_{PANIeb}/R_{CNT} > 1$, $R_{CNT}/R_{PANIeb} + 1 \approx 1$), resulting in a larger contribution from S_{CNT} and making $S_{composite}$ gradually approach S_{CNT}. Because the relative magnitude of thermopower is $S_{PANIeb} > S_{composite} > S_{CNT}$, the decreasing thermopower was observed with higher CNT concentrations. Note that the thermopower of a PANIeb only sample was not measured due to its large electrical resistance in our experiments, but it was estimated to be on the order of hundreds μV/K.[2,44] When $R_{CNT} \ll R_{PANIeb}$, $S_{composite} \approx S_{CNT}$. Therefore, the thermopower of the PANIeb composite with 83.3-wt % S/DWCNTs is almost equal to that of the S/DWCNTs only sample.

When we used electrically more conducting CSA-doped PANI, the electrical conductivity of the PANI-CSA composite containing 50-wt % S/DWCNTs was measured to be ~40 S/cm (Figure 3c), which is approximately 1 order of magnitude higher than that of the PANIeb composite. We believe that the higher conductivity comes from the improved charge transport at the junctions between CNTs, as illustrated in the inset of Figure 3d. The electrical conductivity of PANI-CSA and PANIeb composites with 50 wt % S/DWCNTs could be estimated by using a parallel resistor model

$$\sigma_{composite} = V_{PANI}\sigma_{PANI} + V_{CNT}\sigma_{CNT} \quad (2)$$

where σ and V are electrical conductivity and volume fraction of the indexed material, respectively. Assuming PANI-CSA and

DOI: 10.1021/acsami.5b01149
ACS Appl. Mater. Interfaces 2015, 7, 9589−9597

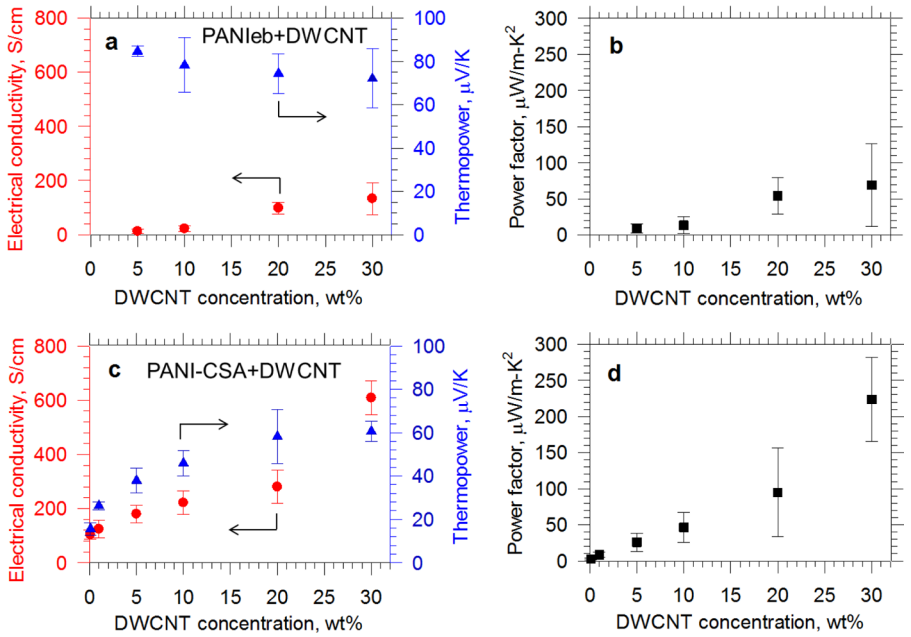

Figure 4. Electrical conductivity and thermopower of (a) PANIeb composites (Sample 9–12) and (c) PANI-CSA composites (Sample 13–18) containing various amounts of DWCNTs. The corresponding power factors for (b) PANIeb composites and (d) PANI-CSA composites.

PANIeb has the same mass density[45] of 1.3 g/cm^3, and CNT has a mass density[46] of 1.6 g/cm^3, the volume fractions of polymers and CNT are 0.55 and 0.45, respectively. With the electrical conductivities of individual materials, PANI-CSA (~57 S/cm), PANIeb (~1×10^{-8} S/cm),[2] and CNTs (~35 S/cm), the electrical conductivity of the PANI-CSA composite is calculated to be ~47 S/cm, which is close to the experimental value (~40 S/cm). However, according to eq 2, the PANIeb composite has much larger electrical conductivity (~16 S/cm) than the experimental value (~4.7 S/cm). The matching theoretical and experimental values from the PANI-CSA composite indicate good charge transport at the junctions between CNTs. This may also be due to the higher packing density of the PANI-CSA composite compared to the PANIeb composite, as shown in Figure 2a, b.

As the concentration of S/DWCNTs was raised from 9.1 to 66.7 wt %, the electrical conductivity was increased from ~21 to ~49 S/cm. Interestingly, the electrical conductivity of PANI-CSA (i.e., 0-wt % S/DWCNT; see Figure 3c) was measured to be 57 S/cm, which is higher than those of CNT-containing composites. This could be attributed to the lower conductivity (~35 S/cm) of the CNT only sample (see Figure 3a), compared to PANI-CSA. In the PANI-CSA composities, we believe the electrical contact resistance between the nanotubes was lowered by introducing the conducting polymer. In CNT-only samples, cylindrical CNTs make either point-to-point or line-to-line contacts, resulting in small contact areas and leaving voids in the samples.[22] In contrast, it is hard to see voids in the PANI composites (particularly PANI-CSA composites, as shown in Figure 2) The polymer can lower contact resistance by enlarging the contact surface area. The conducting polymer can also bind the nanotubes stronger and thereby increase the packing density. In addition, PANI may alleviate the interference from electrically insulating SDBS and *m*-cresol in the composite.

On the other hand, the thermopower of Sample 8 (PANI-CSA with 66.7-wt % S/DWCNTs) was higher than those of the CNT only and PANI-CSA only samples, resulting in an improved power factor (Figure 3d). The typical thermopower behaviors were reversed for the PANI-CSA composites, showing larger thermopower with higher electrical conductivity (Sample 4–8 in Figure 3c). When the concentration of S/DWCNTs is 9.1 wt % (Sample 4), the thermopower is ~26 μV/K with ~21 S/cm. With a higher 66.7-wt % S/DWCNT concentration, the thermopower of the composite reached ~85 μV/K with a higher electrical conductivity, ~47 S/cm. It is interesting to see that this thermopower is larger than those of individual components (~54 μV/K for S/DWCNTs and ~18 μV/K for PANI-CSA[2]). Steep increases of the power factor from the PANI-CSA composites were observed due to the simultaneous improvement in both electrical conductivity and thermopower, resulting in ~34 μW/(m K^2) with 66.7 wt % of S/DWCNTs from ~1.5 μW/(m K^2) with 9.1 wt % of S/DWCNTs.

We also tested electrically more conductive DWCNTs[22] instead of S/DWCNTs to further improve the power factor (Figure 4). This CNT replacement indeed significantly raised the electrical conductivity of the PANI-CSA composites up to ~610 S/cm with 30 wt % DWCNTs (Sample 18), as shown in Figure 4b. The PANIeb counterpart (Sample 12), on the other hand, resulted in ~133 S/cm (Figure 4a), which is lower than that of the PANI-CSA composite, presumably due to the low electrical conductivity of PANIeb. Both thermopower and electrical conductivity of the PANI-CSA composites with DWCNTs (Sample 13–18) increased with higher CNT concentrations, which is opposite to the behaviors of the PANIeb composites (Sample 9–12). The power factor of the PANI-CSA composites containing DWCNTs reached ~220 μW/(m K^2) at room temperature, which is more than 2 orders of magnitude higher compared to PANI-CSA as well as the highest among previously reported PANI composites. This value is 1 order of magnitude higher than a PANI-CNT composite (20 μW/(m K^2)) with a higher CNT concentration (41 wt %),[33] and higher than a highly ordered PANI-CNT composite (176 μW/(m K^2)) with an even higher CNT concentration (~71 wt %).[34]

DOI: 10.1021/acsami.5b01149
ACS Appl. Mater. Interfaces 2015, 7, 9589–9597

The simultaneous increase of electrical conductivity and thermopower has been further investigated by carrying out the Hall measurements to obtain the electronic carrier mobility and concentration. As shown in Figure 5, when DWCNTs were

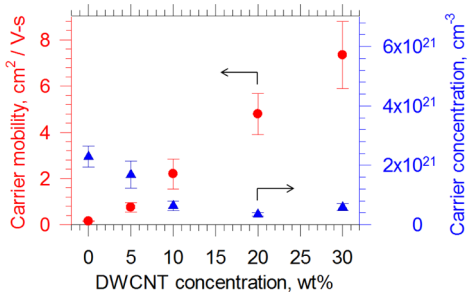

Figure 5. Hole carrier mobility and carrier concentration of PANI-CSA composites at different DWCNT wt %.

added to PANI-CSA, the carrier mobility was significantly increased to ~7.3 cm^2/(V s) from ~0.15 cm^2/(V s) of PANI-CSA and the carrier concentration was reduced. The relatively larger increase in the mobility (μ) compared to the reduction in the carrier concentration (n) can be attributed to the increasing electrical conductivity with addition of DWCNTs since electrical conductivity (σ) has the following relation, $\sigma = \mu ne$, where n and e stand for electronic carrier concentration and electron charge. The different trends of the PANI-CSA/DWCNTs and PANIeb/DWCNTs composites could be attributed to changes in the carrier mobility and concentration as a function of CNT concentration. For PANI-CSA, the addition of DWCNTs remarkably raised the carrier mobility from ~0.15 to ~7.3 cm^2/(V s) (~50 time improvement) and decreased the carrier concentration from ~2.1 × 10^{21} to ~5.6 × 10^{20} cm^{-3} (~4 time reduction). We believe that the larger improvement in mobility compared to the reduction of the carrier concentration increased electrical conductivity while the reduced carrier concentration played a role in enlarging thermopower. On the other hand, the carrier concentration of the PANIeb composites increases with addition of DWCNTs since the carrier concentration of PANIeb is much lower (≲1 × 10^{17} cm^{-3})[2] than that of DWCNTs (~5 × 10^{20} cm^{-3}, see the texts below), suppressing thermopower.

The improved mobility with DWCNTs was further studied by finding the locations of the Fermi level as well as HOMO and LUMO. The Fermi levels of the DWCNT only and PANI-CSA only samples were found to be 5.01 and 4.81 eV, respectively (Figure 6b). With the addition of DWCNTs, the Fermi level of the PANI-CSA "composites" approached that of DWCNTs. For individual PANI-CSA and DWCNTs (before they were made into composites), the electronic band diagrams are shown in Figure 6c. In PANI-CSA composites, PANI-CSA and DWCNTs were brought into contact, and then we speculate that band bending in the HOMO and LUMO of PANI-CSA occurs to equilibrate the Fermi levels, as shown in Figure 6d. In this band alignment, the hole carriers in PANI-CSA are likely to be attracted to the Fermi level of DWCNT whose electronic mobility is much higher than that of the PANI-CSA only sample. The mobility of DWCNTs can be estimated from $\mu = \sigma/(ne)$. Electrical conductivity of the same DWCNTs (the same production batch) without intense doping processes is ~1 × 10^5 S/m,[22] and the carrier concentration is expected to be ~5 × 10^{20} cm^{-3} from Figure 5. Therefore, the mobility of DWCNTs can be estimated to be on the order of

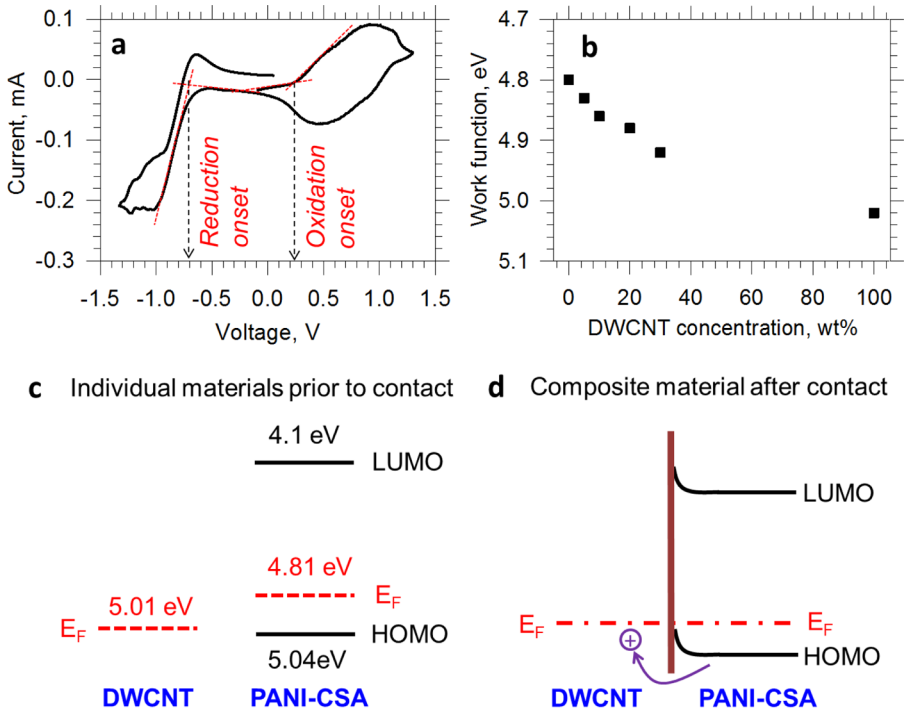

Figure 6. (a) Cyclic voltammogram of PANI-CSA composites, showing the oxidation and reduction onset potentials with respect to Ag/Ag$^+$. (b) Work function of PANI-CSA composites at different DWCNT concentrations and a DWCNT only sample. (c) Fermi level of DWCNT only and PANI-CSA only samples, and HOMO and LUMO of the PANI-CSA only sample. (d) Fermi level, HOMO, and LUMO when DWCNTs and PANI-CSA were made into composites. It should be noted that c represents electronic bands of the individual materials before they were brought into contact, whereas d represents those after contact in composites.

DOI: 10.1021/acsami.5b01149
ACS Appl. Mater. Interfaces 2015, 7, 9589−9597

10 $cm^2/(V\ s)$, which is close to the projected mobility value with 100-wt % DWCNTs in Figure 5.

The increasing thermopower behavior could be explained on the basis of the following relation that one can derive from the general thermopower (S) expression[23] for degenerate semiconductors or metals when energy (E) is proportional to E^r and parabolic electronic bands are assumed.

$$|S| = \frac{\pi^2 k_B}{3e}\left(\frac{2m^* k_B T}{\hbar^2(3\pi^2 n)^{2/3}}\right)\left(\frac{3}{2} + r\right) \quad (3)$$

where k_B, m^*, T, and r are the Boltzmann constant, effective electron mass, absolute temperature, and scattering parameter, respectively. For a given temperature and a fixed scattering parameter, thermopower is a sole function of $n^{-2/3}$, and therefore the reduction in the carrier concentration is expected to increase thermopower because of the inversely proportional relation. To fully characterize the thermoelectric figure-of-merit, the thermal conductivity of the samples needs to be measured but it is difficult to accurately measure the thermal conductivity of our thin samples along the in-plane direction. Note that all the electrical properties were measured along the in-plane direction.

We noticed that recent papers[33,34] used out-of-plane thermal conductivities (along the thickness direction) of PANI composites to calculate thermoelectric figure-of-merit (ZT) although the electrical properties were measured along the in-plane direction. Oddly, the thermal conductivity of a PANI composite containing 71 wt % CNT (0.43 W/(m K)) was reported to be lower than that of a 41 wt % composite (1.5 W/(m K)). According to recent studies,[47,48] the out-of-plane thermal conductivity of conducting polymers is significantly lower than that of the in-plane thermal conductivity. This is mainly because electrical conduction along the in-plane direction is better than the out-of-plane. In fact, electronic thermal conductivity based on the Wiedemann–Franz law is calculated to be 0.51 W/(m K) from 700 S/cm of the 71 wt % CNT sample, which is higher than their measured value (0.43 W/(m K)) that includes both electronic and lattice thermal conductivity.[34]

Here our samples are not thick enough to characterize thermal conductivity in the in-plane direction. Therefore, we theoretically estimated the thermal conductivity of the composite composed of PANI and 30% CNT using a parallel resistor model:[31]

$$k_{composite} = V_{CNT}k_{CNT} + V_{PANI}k_{PANI} + k_{electron} \quad (4)$$

where k and V respectively indicate thermal conductivity and volume fraction of the indexed material. The densities of CNT and PANI were assumed to be 1.6 and 1.3 g/cm^3, respectively.[45,46] Here we used V_{CNT} = 0.26, V_{PANI} = 0.74, k_{PANI} = 0.2 W/m-K,[49] and k_e = 0.45 W/m-K based on the Wiedemann–Franz law. k_{CNT} was calculated based on a 3D model derived by numerical calculation combined with analytic expression.[31,50] The average length and diameter of individual CNT were determined to be 1.25 μm and 3 nm, respectively.[22,30] It should be noted that the model assumes the infinite thermal conductivity for individual CNT because it is well-known that the thermal contact resistance at CNT-CNT junctions governs macroscopic thermal conduction in CNT composites rather than the intrinsic thermal conductivity of individual CNTs.[20,31,51]

Figure 7 shows the thermal conductivity of PANI-CSA with 30-wt % DWCNTs as a function of thermal contact

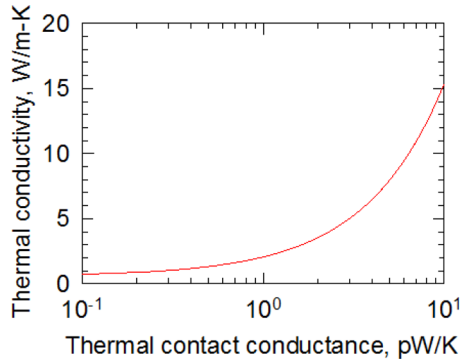

Figure 7. Theoretical thermal conductivity of a PANI-CSA composite with 30 wt % DWCNTs when thermal contact conductance between CNTs varies from 0.1 to 10 pW/K. It was assumed that CNTs are randomly embedded in 3D space of the composite.

conductance between CNTs. We assumed that the maximum thermal contact conductance is 10 pW/K, which corresponds to direct CNT-to-CNT contact without any molecules in between.[52−55] The upper bound of the thermal conductivity is estimated to be 15 Wm-K and the lower bound is 0.7 W/(m K) with the minimum thermal contact conductance of 0.1 pW/K in the case of CNT junctions intervened by polymers.[31] Therefore, we estimated that the highest ZT value from our samples is ~0.1 at room temperature.

4. CONCLUSION

In summary, PANI-CNT composites were synthesized by combining either PANIeb or PANI-CSA with either S/DWCNTs or DWCNTs. CNT concentrations were varied and electrical conductivity and thermopower were measured. Composites with PANI-CSA and DWCNT had higher electrical conductivities compared to composites with PANIeb and S/DWCNT, and, with increasing CNT concentrations in PANI-CSA composites, both electrical conductivity and thermopower were simutaneously increased, showing extraordinary electronic transport behaviors. The electrical conductivity of PANI-CSA composites containing 30 wt % DWCNTs was measured to be ~610 S/cm with a thermopower value, ~61 μV/K at room temperature, resulting in more than 2 orders of magnitude higher power factor, ~220 $\mu W/(m\ K^2)$ compared to ~1.8 $\mu W/(m\ K^2)$ of PANI-CSA. This value is also the highest among those of the previously reported PANI composites. We believe that the simultaneous improvement in electrical conductivity and thermopower could be attributed to the increase of the electronic carrier mobility and the reduction of the carrier concentration. This study identified a promising method of achieving high-performance fully organic thermoelectric composites with unique characteristics such as flexibility and low density that are not easily achievable with inorganic thermoelectric materials.

AUTHOR INFORMATION

Corresponding Author

*E-mail: chyu@tamu.edu. Tel: 979-862-1073. Fax: 979-845-3081.

Notes

The authors declare no competing financial interest.

DOI: 10.1021/acsami.5b01149
ACS Appl. Mater. Interfaces 2015, 7, 9589−9597

■ ACKNOWLEDGMENTS

The authors gratefully acknowledge financial supports from the US Air Force Office of Scientific Research (FA9550-09-1-0609) under the auspices of Dr. Charles Lee, and the Pioneer Research Center Program through the National Research Foundation of Korea (2011-0001645) funded by the Ministry of Education, Science and Technology.

■ REFERENCES

(1) Rowe, D. M. *CRC Handbook of Thermoelectrics*; CRC Press: Boca Raton, FL, 1995.
(2) Wang, H.; Yin, L.; Pu, X.; Yu, C. Facile Charge Carrier Adjustment for Improving Thermopower of Doped Polyaniline. *Polymer* **2013**, *54*, 1136−1140.
(3) Liu, H.; Hu, X. B.; Wang, J. Y.; Boughton, R. I. Structure, Conductivity, and Thermopower of Crystalline Polyaniline Synthesized by the Ultrasonic Irradiation Polymerization Method. *Macromolecules* **2002**, *35*, 9414−9419.
(4) Park, Y. W.; Lee, Y. S.; Park, C.; Shacklette, L. W.; Baughman, R. H. Thermophower and Conductivity of Metallic Polyaniline. *Solid State Commun.* **1987**, *63*, 1063−1066.
(5) Toshima, N. Conductive polymers as a new type of thermoelectric material. *Macromol. Symp.* **2002**, *186*, 81−86.
(6) Yakuphanoglu, F.; Senkal, B. F.; Sarac, A. Electrical Conductivity, Thermoelectric Power, and Optical Properties of Organo-Soluble Polyaniline Organic Semiconductor. *J. Electron. Mater.* **2008**, *37*, 930−934.
(7) Yan, H.; Toshima, N. Thermoelectric Properties of Alternatively Layered Films of Polyaniline and Camphorsulfonic Acid Doped Polyaniline. *Chem. Lett.* **1999**, 1217−1218.
(8) Wang, Y. Y.; Cai, K. F.; Yin, J. L.; An, B. J.; Du, Y.; Yao, X. In Situ Fabrication and Thermoelectric Properties of PbTe-Polyaniline Composite Nanostructures. *J. Nanopart. Res.* **2011**, *13* (2), 533−539.
(9) Toshima, N.; Jiravanichanun, N.; Marutani, H. Organic Thermoelectric Materials Composed of Conducting Polymers and Metal Nanoparticles. *J. Electron. Mater.* **2012**, *41* (6), 1735−1742.
(10) Su, L.; Gan, Y. X. Experimental Study on Synthesizing TiO2 Nanotube/Polyaniline (PANI) Nanocomposites and Their Thermoelectric and Photosensitive Property Characterization. *Composites, Part B* **2012**, *43* (2), 170−182.
(11) Toshima, N.; Imai, M.; Ichikawa, S. Organic-Inorganic Nanohybrids as Novel Thermoelectric Materials: Hybrids of Polyaniline and Bismuth(III) Telluride Nanoparticles. *J. Electron. Mater.* **2011**, *40* (5), 898−902.
(12) Chatterjee, K.; Ganguly, S.; Kargupta, K.; Banerjee, D. Bismuth Nitrate Doped Polyaniline. Characterization and Properties for Thermoelectric Application. *Synth. Met.* **2011**, *161* (3−4), 275−279.
(13) Bo, X.; Yang, Y.; Zhang, J. Electrodeposition and Thermoelectric Properties of Bi2Te3 Films on the Conducting Polyaniline Film Electrode. *Cailiao Yanjiu Xuebao* **2008**, *22* (6), 645−650.
(14) Choi, K.; Yu, C. Highly Doped Carbon Nanotubes with Gold Nanoparticles and Their Influence on Electrical Conductivity and Thermopower of Nanocomposites. *PLoS One* **2012**, *7* (9), e44977.
(15) Liu, J.; Sun, J.; Gao, L. Flexible Single-Walled Carbon Nanotubes/Polyaniline Composite Films and Their Enhanced Thermoelectric Properties. *Nanoscale* **2011**, *3*, 3616−3619.
(16) Wang, Q.; Yao, Q.; Chang, J.; Chen, L. Enhanced Thermoelectric Properties of CNT/PANI Composite Nanofibers by Highly Orienting the Arrangement of Polymer Chains. *J. Mater. Chem.* **2012**, *22*, 17612−17618.
(17) Xiang, J.; Drzal, L. T. Templated Growth of Polyaniline on Exfoliated Graphene Nanoplatelets (GNP) and Its Thermoelectric Properties. *Polymer* **2012**, *53* (19), 4202−4210.
(18) Zhao, Y.; Tang, G.-S.; Yu, Z.-Z.; Qi, J.-S. The Effect of Graphite Oxide on the Thermoelectric Properties of Polyaniline. *Carbon* **2012**, *50* (8), 3064−3073.
(19) Narayanunni, V.; Gu, H.; Yu, C. Monte Carlo Simulation for Investigating Influence of Junction and Nanofiber Properties on Electrical Conductivity of Segregated-Network Nanocomposites. *Acta Mater.* **2011**, *59*, 4548−4555.
(20) Yu, C.; Kim, Y. S.; Kim, D.; Grunlan, J. C. Thermoelectric Behavior of Segregated-Network Polymer Nanocomposites. *Nano Lett.* **2008**, *8*, 4428.
(21) Ryu, Y.; Freeman, D.; Yu, C. High Electrical Conductivity and N-type Thermopower From Double-/Single-wall Carbon Nanotubes by Manipulating Charge Interactions Between Nanotubes and Organic/Inorganic Nanomaterials. *Carbon* **2011**, *49*, 4745−4751.
(22) Ryu, Y.; Yin, L.; Yu, C. Dramatic Electrical Conductivity Improvement of Carbon Nanotube Networks by Simultaneous Debundling and Hole-doping with Chlorosulfonic Acid. *J. Mater. Chem.* **2012**, *22*, 6959−6964.
(23) Yu, C.; Ryu, Y.; Yin, L.; Yang, H. Modulating electronic transport properties of carbon nanotubes and improving the thermoelectric power factor via nanoparticle decoration. *ACS Nano* **2011**, *5*, 1297−1303.
(24) Ryu, Y.; Yu, C. The Influence of Incorporating Organic Molecules or Inorganic Nanoparticles on the Optical and Electrical Properties of Carbon Nanotube Films. *Solid State Commun.* **2011**, *151*, 1932−1935.
(25) Freeman, D.; Choi, K.; Yu, C. N-Type Thermoelectric Performance of Functionalized Carbon Nanotube-Filled Polymer Composites. *PLoS One* **2012**, *7*, e47822.
(26) Yu, C.; Murali, A.; Choi, K.; Ryu, Y. Air-Stable Fabric Thermoelectric Modules Made of N- and P-type Carbon Nanotubes. *Energy Environ. Sci.* **2012**, *5*, 9481−9486.
(27) Kim, S. L.; C, K.; Tazebay, A.; Yu, C. Flexible Power Fabrics Made of Carbon Nanotubes for Harvesting Thermoelectricity. *ACS Nano* **2014**, *8*, 2377−2386.
(28) Kim, D.; Kim, Y.; Choi, K.; Grunlan, J. C.; Yu, C. Improved Thermoelectric Behavior of Nanotube-Filled Polymer Composites with Poly(3,4-ethylenedioxythiophene) Poly(styrenesulfonate). *ACS Nano* **2010**, *4*, 513−523.
(29) Kim, Y. S.; Kim, D.; Martin, K. J.; Yu, C.; Grunlan, J. C. Influence of Stabilizer Concentration on Transport Behavior and Thermopower of Carbon Nanotube Filled Latex-Based Composites. *Macromol. Mater. Eng.* **2010**, *295*, 431−436.
(30) Moriarty, G. P.; Briggs, K.; Stevens, B.; Yu, C.; Grunlan, J. C. Fully Organic Nanocomposites with High Thermoelectric Power Factors by using a Dual-Stabilizer Preparation. *Energy Technol.* **2013**, *1* (4), 265−272.
(31) Yu, C.; Choi, K.; Yin, L.; Grunlan, J. C. Light-Weight Flexible Carbon Nanotube Based Organic Composites with Large Thermoelectric Power Factors. *ACS Nano* **2011**, *5*, 7885−7892.
(32) Meng, C.; Liu, C.; Fan, S. A Promising Approach to Enhanced Thermoelectric Properties Using Carbon Nanotube Networks. *Adv. Mater.* **2010**, *22*, 535−539.
(33) Yao, Q.; Chen, L.; Zhang, W.; Liufu, S.; Chen, X. Enhanced Thermoelectric Performance of Single-Walled Carbon Nanotubes/Polyaniline Hybrid Nanocomposites. *ACS Nano* **2010**, *4*, 2445−2451.
(34) Yao, Q.; Wang, Q.; Wang, L.; Chen, L. Abnormally Enhanced Thermoelectric Transport Properties of SWNT/PANI Hybrid Films by the Strengthened PANI Molecular Ordering. *Energy Environ. Sci.* **2014**, *7* (11), 3801−3807.
(35) Sakkopoulos, S.; Vitoratos, E.; Dalas, E.; Pandis, G.; Tsamourast, D. Thermopower Sign Reversal Versus Temperature and DC Conductivity in Polyaniline Derivatives. *J. Phys.: Condens. Matter* **1992**, *4*, 2231−2237.
(36) Cardoso, M. J. R.; Lima, M. F. S.; Lenz, D. M. Polyaniline Synthesized with Functionalized Sulfonic Acids for Blends Manufacture. *Mater. Res.* **2007**, *10*, 425−429.
(37) Kumari, K.; Ali, V.; Kumar, A.; Kumar, S.; Zulfequar, M. D.C. Conductivity and Spectroscopic Studies of Polyaniline Doped with Binary Dopant ZrOCl2/AgI. *Bull. Mater. Sci.* **2011**, *34* (6), 1237−1243.
(38) Wang, Y. Y.; Cai, K. F.; Yin, J. L.; Du, Y.; Yao, X. One-pot Fabrication and Thermoelectric Properties of Ag2Te-Polyaniline

DOI: 10.1021/acsami.5b01149
ACS Appl. Mater. Interfaces 2015, 7, 9589−9597

Core−Shell Nanostructures. *Mater. Chem. Phys.* **2012**, *133* (2−3), 808−812.
(39) Zhang, K.; Davis, M.; Qiu, J.; Hope-Weeks, L.; Wang, S. Thermoelectric Properties of Porous Multi-walled Carbon Nanotube/Polyaniline Core/Shell Nanocomposites. *Nanotechnology* **2012**, *23* (38), 385701−385708.
(40) Wang, L.; Yao, Q.; Bi, H.; Huang, F.; Wang, Q.; Chen, L. PANI/Graphene Nanocomposite Films with High Thermoelectric Properties by Enhanced Molecular Ordering. *J. Mater. Chem. A* **2015**, *3* (13), 7086−7092.
(41) Yan, H.; Kou, K. Enhanced Thermoelectric Properties in Polyaniline Composites with Polyaniline-Coated Carbon Nanotubes. *J. Mater. Sci.* **2014**, *49* (3), 1222−1228.
(42) Liu, J.; Yu, H.-Q. Thermoelectric Enhancement in Polyaniline Composites with Polypyrrole-Functionalized Multiwall Carbon Nanotubes. *J. Electron. Mater.* **2014**, *43* (4), 1181−1187.
(43) Chatterjee, K.; Mitra, M.; Kargupta, K.; Ganguly, S.; Banerjee, D., Synthesis, Characterization and Enhanced Thermoelectric Performance of Structurally Ordered Cable-Like Novel Polyaniline-Bismuth Telluride Nanocomposite. *Nanotechnology* **2013**, *24* (21), 215703/1−215703/10, 10 pp.
(44) Mateeva, N.; Niculescu, H.; Schlenoff, J.; Testardi, L. R. Correlation of Seebeck Coefficient and Electric Conductivity in Polyaniline and Polypyrrole. *J. Appl. Phys.* **1998**, *83*, 3111−3117.
(45) Skotheim, T. A.; Elsenbaumer, R. L.; Reynolds, J. R., Handbook of Conducting Polymers. Marcel Dekker: New York, 1998.
(46) Ci, L.; Vajtai, R.; Ajayan, P. M. Vertically Aligned Large-Diameter Double-Walled Carbon Nanotube Arrays Having Ultralow Density. *J. Phys. Chem. C* **2007**, *111*, 9077−9080.
(47) Liu, J.; Wang, X.; Li, D.; Coates, N. E.; Segalman, R. A.; Cahill, D. G. Thermal Conductivity and Elastic Constants of PEDOT:PSS with High Electrical Conductivity. *Macromolecules* **2015**, *48* (3), 585−591.
(48) Weathers, A.; Khan, Z. U.; Brooke, R.; Evans, D.; Pettes, M. T.; Andreasen, J. W.; Crispin, X.; Shi, L. Significant Electronic Thermal Transport in the Conducting Polymer Poly(3,4-ethylenedioxythiophene). *Adv. Mater.* **2015**, *27* (12), 2101−2106.
(49) Yan, H.; Ohno, N.; Toshima, N. Low Thermal Conductivities of Undoped and Various Protonic Acid-Doped Polyaniline Films. *Chem. Lett.* **2000**, *29* (4), 392−393.
(50) Volkov, A. N.; Zhigilei, L. V. Scaling Laws and Mesoscopic Modeling of Thermal Conductivity in Carbon Nanotube Materials. *Phys. Rev. Lett.* **2010**, *104* (21), 215902.
(51) Hone, J.; Whitney, M.; Piskoti, C.; Zettl, A. Thermal Conductivity of Single-Walled Carbon Nanotubes. *Phys. Rev. B* **1999**, *59* (4), R2514−R2516.
(52) Chalopin, Y.; Volz, S.; Mingo, N. Upper Bound to the Thermal Conductivity of Carbon Nanotube Pellets. *J. Appl. Phys.* **2009**, *105* (8), 084301.
(53) Zhong, H.; Lukes, J. R. Interfacial Thermal Resistance between Carbon Nanotubes: Molecular Dynamics Simulations and Analytical Thermal Modeling. *Phys. Rev. B* **2006**, *74* (12), 125403.
(54) Prasher, R. S.; Hu, X. J.; Chalopin, Y.; Mingo, N.; Lofgreen, K.; Volz, S.; Cleri, F.; Keblinski, P. Turning Carbon Nanotubes from Exceptional Heat Conductors into Insulators. *Phys. Rev. Lett.* **2009**, *102* (10), 105901.
(55) Estrada, D.; Pop, E. Imaging Dissipation and Hot Spots in Carbon Nanotube Network Transistors. *Appl. Phys. Lett.* **2011**, *98* (7), 073102.

DOI: 10.1021/acsami.5b01149
ACS Appl. Mater. Interfaces 2015, 7, 9589−9597